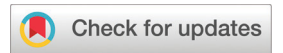
Dalton Transactions



PAPER



Cite this: *Dalton Trans.*, 2021, **50**, 4936

Received 2nd March 2021, Accepted 19th March 2021 DOI: 10.1039/d1dt00707f

rsc.li/dalton

A unique series of chromium(III) mono-alkynyl complexes supported by tetraazamacrocycles†

Ashley J. Schuman, Sarah F. T. Robey, Eileen C. Judkins, Matthias Zeller and Tong Ren **

Described herein is the synthesis and characterization of macrocyclic Cr^{III} mono-alkynyl complexes. By using the *meso*-form of the tetraazamacrocycle HMC (HMC = 5,5,7,12,12,14-hexamethyl-1,4,8,11-tetraazacyclotetradecane), trans-[$Cr(HMC)(C_2Ph)Cl]OTf$ (**1a**), trans-[$Cr(HMC)(C_2Np)Cl]OTf$ (**2a**), trans-[$Cr(HMC)(C_2Ph)Cl]OTf$ (**1a**), trans-[$Cr(HMC)(C_2Np)Cl]OTf$ (**2a**), trans-[$Cr(HMC)(C_2C_6H_3))Cl]OTf$ (**4a**) complexes have been realized. These complexes were synthesized in high yield through the reaction of trans-[Cr(meso-HMC)($C_2Ar)_2$]OTf (**1b**-**4b**) with stoichiometric amounts of methanolic HCl. Single crystal X-ray diffraction showed that the trans-stereochemistry and pseudo-octahedral geometry is retained in the desired mono-alkynyl complexes. The absorption spectra of complexes **1a**-**4a** display d-d bands with distinct vibronic progressions that are slightly red shifted from trans-[$Cr(HMC)(C_2Ar)_2$]+ with approximately halved molar extinction coefficients. Time-delayed measurements of the emission spectra for complexes **1a**-**4a** at 77 K revealed phosphorescence with lifetimes ranging between 343 μ s (**4a**) and 397 μ s (**1a**). The phosphorescence spectra of **1a**-**4a** also exhibit more structuring than the bis-alkynyl complexes due to a strengthened vibronic coupling between the Cr^{III} metal center and alkynyl ligands.

Introduction

Transition-metal alkynyl chemistry is a fascinating topic in the realms of both synthesis and materials applications. ¹⁻³ Weinstein and co-workers have garnered attention for the study of donor-bridge-acceptor (D−B−A) complexes utilizing a *trans*-Pt^{II}-bis-alkynyl bridge, and demonstrated that the evolution of photoinduced electron transfer (PET) excited states, especially the formation of the charge-separated (CS) state, can be attenuated by vibrational excitation of the Pt bound C≡C bonds. ⁴ Expanding this chemistry to include earth abundant 3d metal complexes and investigating their PET processes is paramount in creating sustainable materials for optoelectronic applications. To accomplish this, D−B−A type complexes with dissymmetric alkynyl ligands need to be realized.

In the preparation of dissymmetric alkynyl D-B-A complexes, a mono-alkynyl species is first synthesized. ^{5,6} Using this stepwise approach, it is possible to investigate the properties of each independent unit (D-B, B-A), the dissymmetric complex (D-B-A), and the symmetric complexes (D-B-D, A-B-

Department of Chemistry, Purdue University, West Lafayette, Indiana 47907, USA. E-mail: tren@purdue.edu

 \dagger Electronic supplementary information (ESI) available. CCDC 2067384–2067389. For ESI and crystallographic data in CIF or other electronic format see DOI: 10.1039/d1dt00707f

A). Selective synthesis of mono-alkynyl species of $\mathrm{Co^{III}}(\mathrm{cyclam})$ complexes was first reported by Shores, which proceeded under the weak base conditions. Our laboratory has published several examples of dissymmetric alkynyl complexes with $\mathrm{Ru_2}$ and $\mathrm{Co^{III}}(\mathrm{cyclam})$ metal centers. Femtosecond transient absorption and time-resolved IR spectroscopic studies of [Co (cyclam)($\mathrm{C_2NAP^{iPr}})(\mathrm{C_2D})$] complexes ($\mathrm{C_2NAP^{iPr}}$ = 4-ethynyl-*N*-ispropyl-1,8-napthalimide, $\mathrm{D} = \mathrm{C_6H_4}$ -4-NMe₂, Ph, or $\mathrm{C_6H_4}$ -4-N (4-MeOPh)₂), revealed the formation of desirable CS states, which were quickly deactivated by the low-lying Co-centered triplet states. This necessitates further investigation of other macrocyclic 3d metal alkynyl bridges that sustain long-lived CS and metal-to-ligand charge transfer states.

Macrocyclic chromium alkynyl chemistry emerged with Taube and coworkers' $[Cr^{III}(phthalocyanine)(C_2Ph)_2]^-$ complex. ¹² Following this, Berben and Long reported several $Cr^{III}(Me_3TACN)(C_2R)_3$ type complexes $(Me_3TACN = N,N',N''$ -trimethyl-1,4,7-triazacyclononane, $R = C_2SiMe_3$, C_2H , C_4SiMe_3 , and C_4H), ¹³ and $Cr^{III}(cyclam)$ alkynyl complexes, trans- $[Cr(cyclam)(C_2R)_2]^+$ $(R = C_2SiMe_3, C_2H)$ and trans- $[Cr(cyclam)(1,3-C_2C_6H_4C_2H)_2]^+$. ¹⁴ Additional $Cr^{III}(cyclam)$ alkynyl complexes have been documented by the groups of Wagenknecht, ¹⁵ Nishijo, ¹⁶⁻¹⁹ and Ren. ²⁰ Recent explorations of macrocyclic chromium alkynyl chemistry in our group include the study of cis-/trans- $[Cr^{III}(cyclam')(C_2R)_2]^+$ type complexes, where cyclam' is the C-substituted cyclam derivative DMC^{21} (DMC = 5,12-

dimethyl-1,4,8,11-tetraazacyclotetradecane) or HMC (HMC = 5,5,7,12,12,14-hexamethyl-1,4,8,11-tetraazacyclotetradecane). ^{22,23} Thus far, all macrocyclic Cr^{III} alkynyl complexes feature symmetric bis-alkynyl ligands, while D–B–A type complexes have yet to be realized.

Examples of Cr mono-alkynyl complexes are known but sparse. Smith's laboratory synthesized several CpCrIII- $[(ArNCMe)_2CH](R)$ complexes, including $R = C_2H$, in order to study Cr-R bond homolysis (Ar = ortho-disubstituted aryl).²⁴ Earlier work by Smith resulted in CpCr(NO)(NⁱPr₂)(R) type complexes ($R = C_2CMe_3$ and C_2Ph), where the stability of the complexes was attributed to the π -bonding interactions of the $[Cr(NO)(N^{i}Pr_{2})]^{2+}$ core. ²⁵ Two $(\eta^{5}-C_{5}H_{4}R)Cr(NO)_{2}-C_{2}Ph$ complexes (R = H or COOCH₃) were synthesized (via CuI catalyzed coupling) and characterized.26 Berben discovered a unique dinuclear complex trans- $[(Me_3SiCC)(dmpe)_2Cr]_2(\mu-N_2)$ (dmpe = 1,2-bis(dimethylphosphino)ethane) from the reaction between trans-Cr(dmpe)₂Cl₂ and LiCCSiMe₃ under N₂, ²⁷ and analogous compounds were further investigated by Shores.²⁸ Also based on Cr^{II}(dmpe)₂, Berke and coworkers synthesized a series of mono-alkynyl Cr^{II}(dmpe)₂ complexes using trimethylstannyl and sodium alkynyl reagents.^{29,30} Macrocyclic chromium mono-alkynyl complexes have thus far remained elusive. Reported herein are the syntheses and characterizations of a unique series of Cr^{III}(HMC) mono-alkynyl complexes 1a-4a, and new bis-alkynyl complexes 3b and 4b.

Experimental

General methods

Phenylacetylene was purchased from Oakwood Chemical and used without further purification. HMC, ³¹ trans-[Cr(HMC)Cl₂]-Cl/OTf, ³² trans-[Cr(HMC)(C₂Ph)₂]Cl/OTf, ²³ trans-[Cr(HMC)(C₂Np)₂]-Cl/OTf, ²² TMS-C₂Np, ³³ TMS-C₂C₆H₄^tBu, ³⁴ and TMS-C₂(3,5-Cl₂C₆H₃) ³⁵ were prepared according to literature procedures. Tetrahydrofuran was freshly distilled over Na/benzophenone. The preparation of bis-alkynyl complexes **1b** and **2b** was performed under a dry N₂ atmosphere using standard Schlenk procedures, ^{21,23} and new complexes **3b** and **4b** were synthesized similarly. Preparation of mono-alkynyl complexes **1a–4a** was carried out under ambient conditions. Unless specified, the counter anion is always triflate (OTf; CF₃SO₃) in this study.

Physical methods

Elemental analysis was performed by Atlantic Microlab, Inc in Norcross, GA. UV-vis spectra were obtained with a JASCO V-670 spectrophotometer in $\mathrm{CH_2Cl_2}$ solutions. Emission data were recorded on a Varian Cary Eclipse fluorescence spectrophotometer. FT-IR spectra were measured as neat samples with a JASCO FT/IR-6300 spectrometer equipped with an ATR accessory. ESI-MS were analyzed on an Advion Mass Spectrometer. Magnetic susceptibility was calculated *via* the Evans method³⁶ using ¹H NMR spectra that were recorded on a Varian Inova 300 spectrometer operating at 300 MHz. Single crystal X-ray

diffraction data were collected on Nonius Kappa CCD and Bruker Quest instruments as detailed in the SI.

Synthesis

trans-[Cr(HMC)(C₂Ph)Cl]OTf (1a). The reaction between 0.070 g (0.11 mmol) of trans-[Cr(HMC)(C₂Ph)₂]OTf and 1 equivalent of 0.12 M HCl in CH₃OH yielded a yellow solution, which was stirred for 20 minutes under ambient conditions. Solvent was removed by rotary evaporation, and a yellow solid (0.059 g, 93% based on Cr) was obtained after purification through a silica plug with 1a eluted in 9:1 CH₂Cl₂: CH₃OH. An analogous procedure was used to obtain [1a]Cl from trans-[Cr(HMC)(C₂Ph)₂]Cl, from which a crystal was grown by slow diffusion of Et₂O into CH₃OH. Elem. Anal. Found (Calcd) for trans-[Cr(HMC)(C₂Ph)Cl]OTf·3H₂O: C, 44.8 (44.5); H, 6.6 (6.7); N, 8.5 (8.3). UV-vis, $\lambda_{\text{max}}/\text{nm}$ ($\varepsilon/\text{M}^{-1}$ cm⁻¹): 365 (450), 375 (520), 388 (500), 402 (520), 417sh, 433 (260), 472 (90). FT-IR ν (C=C)/cm⁻¹: 2088w. ESI-MS [M[†]]: 472 m/z for the cationic species [1a]⁺. Magnetic susceptibility, $\mu_{\text{eff}}/\mu_{\text{B}}$: 3.85.

trans-[Cr(HMC)(C₂Np)Cl]OTf (2a). The reaction between trans-[Cr(HMC)(C₂Np)₂]OTf (0.050 g, 0.063 mmol) and 1 equivalent of 0.12 M HCl in 10 mL CH₃OH yielded an orange solution, which was stirred for 20 minutes under ambient conditions. Solvent was removed by rotary evaporation and an orange solid (0.039 g, 92% based on Cr) was obtained after purification through a silica gel plug, eluted with 9:1 CH₂Cl₂: CH₃OH. Single crystals suitable for X-ray diffraction were grown from vapor diffusion of Et₂O into CH₃CN. Elem. Anal. Found (Calcd) for trans-[Cr(HMC)(C₂Np)Cl] OTf-0.5CH₃CN·0.5H₂O: C, 51.5 (51.4); H, 6.6 (6.4); N, 8.9 (9.0). UV-vis, $\lambda_{\text{max}}/\text{nm}$ (ε/M⁻¹ cm⁻¹): 442 (78), 467 (87), 498 (63), 528 (28), 542 (31). FT-IR ν (C=C)/cm⁻¹: 2080w. ESI-MS [M⁺]: 522 m/z for the cationic species [2a]⁺. Magnetic susceptibility, $\mu_{\text{eff}}/\mu_{\text{B}}$: 3.86.

trans-[Cr(HMC)(C₂C₆H₄^tBu)Cl]OTf (3a). The reaction between 0.050 g (0.074 mmol) of trans-[Cr(HMC)(C₂C₆H₄^tBu)₂] OTf and 1 equivalent of 0.12 M HCl in CH₃OH yielded a yellow solution, which was stirred for 20 minutes under ambient conditions. Solvent was removed by rotary evaporation and a yellow solid (0.037 g, 88% based on Cr) was obtained after purification through a silica plug, with 3a eluted with 9:1 CH₂Cl₂: CH₃OH. Single crystals suitable for X-ray diffraction were grown from slow diffusion of Et₂O into CH₃OH. Elem. Anal. Found (Calcd) for trans-[Cr(HMC)(C₂C₆H₄^tBu)Cl]OTf: C, 51.1 (51.4); H, 7.4 (7.3); N, 8.1 (8.3). UV-vis, $\lambda_{\text{max}}/\text{nm}$ (ε/M⁻¹ cm⁻¹): 379 (560), 393 (550), 407 (570), 423 (360), 438 (300). FT-IR ν (C≡C)/cm⁻¹: 2083w. ESI-MS [M⁺]: 528 m/z for the cationic species [3a]⁺. Magnetic susceptibility, $\mu_{\text{eff}}/\mu_{\text{B}}$: 3.86.

trans-[Cr(HMC)($C_2(3,5\text{-Cl}_2C_6H_3)$)Cl]OTf (4a). The reaction between 0.080 g (0.12 mmol) of trans-[Cr(HMC)($C_2(3,5\text{-Cl}_2C_6H_3)$)2]OTf and 1 equivalent of 0.12 M HCl in CH₃OH yielded a golden yellow solution, which was stirred for 20 minutes under ambient conditions. Solvent was removed by rotary evaporation and a golden yellow solid (0.057 g, 85% based on Cr) was obtained after purification through a silica gel plug, with 4a eluting in 9:1 CH₂Cl₂:CH₃OH. Single

Paper Dalton Transactions

crystals suitable for X-ray diffraction were grown from slow diffusion of Et₂O into CH₃CN. Elem. Anal. Found (Calcd) for *trans*-[Cr(HMC)(C₂(3,5-Cl₂C₆H₃))Cl]OTf·1CH₃OH·0.5H₂O: C, 42.85 (42.7); H, 5.9 (6.1); N, 7.8 (7.6). UV-vis, $\lambda_{\text{max}}/\text{nm}$ ($\varepsilon/\text{M}^{-1}$ cm⁻¹): 380 (290), 391 (290), 408 (300), 422sh, 439 (190). FT-IR ν (C=C)/cm⁻¹: 2085w. ESI-MS [M⁺]: 543 m/z for the cationic species [4a]⁺. Magnetic susceptibility, $\mu_{\text{eff}}/\mu_{\text{B}}$: 3.86.

trans- $[Cr(HMC)(C_2C_6H_4^tBu)_2]OTf$ (3b). A suspension of trans-[Cr(HMC)Cl₂]OTf (0.100 g, 0.180 mmol) in 15 mL THF was combined with 3 equivalents of LiC₂C₆H₄^tBu (prepared from 0.543 mmol TMS-C₂C₆H₄^tBu in THF and 0.75 mmol n-BuLi), and the reaction mixture was stirred for 2 hours at room temperature. After quenching the reaction in air, solvent was removed via rotary evaporation. A silica gel plug was used for purification and 3b was eluted with 9:1 CH₂Cl₂: CH₃OH to yield (0.083 g, 58% yield based on Cr). Single crystals suitable for X-ray diffraction were grown from slow diffusion of hexanes into CH2Cl2. Elem. Anal. Found (Calcd) for trans-[Cr(HMC) $(C_2C_6H_4^tBu)_2$ OTf·1.5H₂O·0.5CH₃CN: C, 57.3 (57.1); H, 7.6 (7.6); N, 7.2 (7.1). UV-vis, $\lambda_{\text{max}}/\text{nm}$ ($\varepsilon/\text{M}^{-1}$ cm⁻¹): 366 (1030), 377 (1070), 391 (1030), 404 (1080), 418 (700), 435 (620). FT-IR $\nu(C \equiv C)/\text{cm}^{-1}$: 2082w. ESI-MS [M⁺]: 650 m/z for the cationic species $[3b]^+$. Magnetic susceptibility, $\mu_{\text{eff}}/\mu_{\text{B}}$: 3.89.

trans- $[Cr(HMC)(C_2(3,5-Cl_2C_6H_3))_2]OTf$ (4b). A suspension of trans- $[Cr(HMC)Cl_2]OTf$ (0.35 g, 0.63 mmol) and $HC_2(3,5-$ Cl₂C₆H₃) (0.32 g, 1.9 mmol) in 25 mL THF was combined with 3.8 mL of 0.5 M LDA (1.9 mmol, prepared from the reaction of 0.6 mL diisopropylamine with 1.6 mL n-BuLi in 5.8 mL THF at 77 K), and the reaction mixture was stirred for 2 hours at room temperature. After quenching the reaction in air, solvent was removed via rotary evaporation. A silica gel plug was used for purification and 4b was eluted with 9:1 CH2Cl2:CH3OH (0.213 g, 41% yield based on Cr). Single crystals suitable for X-ray diffraction were grown from slow diffusion of Et₂O into CH₃CN. Elem. Anal. Found (Calcd) for trans-[Cr(HMC)(C₂(3,5- $Cl_2C_6H_3)_2$ OTf: C, 48.0 (48.0); H, 5.1 (5.1); N, 6.8 (6.8). UV-vis, $\lambda_{\text{max}}/\text{nm} \ (\varepsilon/\text{M}^{-1} \ \text{cm}^{-1})$: 374 (540), 391 (450), 406 (490), 419sh, 438 (310). FT-IR $\nu(C \equiv C)/cm^{-1}$: 2079w. ESI-MS [M⁺]: 679 m/z for the cationic species [4b]⁺. Magnetic susceptibility, $\mu_{\text{eff}}/\mu_{\text{B}}$: 3.76.

Results and discussion

Synthesis

As shown in Scheme 1, the reaction between *trans*-[Cr(*meso*-HMC)Cl₂]OTf and three equivalents of the appropriate lithium arylalkynyl produced the bis-alkynyl complexes *trans*-[Cr(HMC)(C₂Ph)₂]OTf (**1b**),²³ *trans*-[Cr(HMC)(C₂Np)₂]OTf (**2b**),²² *trans*-[Cr (HMC)(C₂C₆H₄^tBu)₂]OTf (**3b**), and *trans*-[Cr(HMC)(C₂(3,5-Cl₂C₆H₃))₂]OTf (**4b**). The bis-alkynyl complexes were filtered through Celite and further purified over silica, with yields between 41–73% depending on the nature of arylalkynyl ligand. Mono-alkynyl complexes *trans*-[Cr(HMC)(C₂Ph)Cl]OTf (**1a**), *trans*-[Cr(HMC)(C₂Np)Cl]OTf (**2a**), *trans*-[Cr(HMC)(C₂C₆H₄^tBu)Cl]OTf (**3a**), and *trans*-[Cr(HMC)(C₂(3,5-Cl₂C₆H₃)) Cl]OTf (**4a**) were then synthesized by the reaction of the appro-

Conditions: (i) \sim 3 equiv of LiC₂Ar, THF, RT, 2h, (ii) 1 equiv 0.12 M HCI_(MeOH)

Scheme 1 General synthesis of Cr^{III}(HMC) mono-alkynyl complexes through acid degradation of Cr^{III}(HMC) bis-alkynyl complexes.

priate *trans*-[Cr(HMC)(C₂Ar)₂]OTf with a stoichiometric amount of HCl in CH₃OH. Purification over silica resulted in yields of *trans*-[Cr(HMC)(C₂Ar)Cl]OTf ranging between 85–93%. A one-step synthesis of *trans*-[Cr(HMC)(C₂Ph)Cl]Cl was attempted by combining a substoichiometric amount of LiC₂Ph with *trans*-[Cr(HMC)Cl₂]Cl, however, the yield of *trans*-[Cr(HMC)(C₂Ph)Cl]Cl was <12% based on Cr (see the ESI†). The improved two-step synthesis of 1a resulted in an overall percent yield of 48% (based on Cr in *trans*-[Cr(HMC)Cl₂]OTf), while other arylalkynyl ligands saw overall yields of up to 67%.

Previous studies on the alkynylation of the *cis/trans* isomers of $[Cr(HMC)Cl_2]^+$ have revealed the $[Cr(HMC)(C_2R)_2]^+$ products retain their *cis/trans* stereochemistry (R = Ph, C₂SiMe₃, and Np).^{22,23} This is in contrast to the alkynylation of Cr(cyclam) and Cr(DMC) complexes, which produced a mixture of *cis/trans* products when *cis-*[Cr(cyclam/DMC)Cl₂]⁺ starting material was employed.^{15,21} We attempted to synthesize both *cis-* and *trans-*[Cr(HMC)(C₂Ar)Cl]⁺ complexes, however, the *cis-*complexes were much less stable and often fully degraded to *cis-*[Cr(HMC)Cl₂]Cl in acidified solution. At present, our focus is on the more robust *trans-*[Cr(HMC)(C₂Ar)Cl]OTf complexes.

Like the corresponding bis-alkynyl complexes, monoalkynyl species 1a–4a are paramagnetic with room temperature effective magnetic moments (Evans method) corresponding to S = 3/2. While well resolved 1H NMR spectra for complexes 1a–4a are unattainable, their compositions were analyzed with ESI-MS and elemental analysis.

Molecular structures

Mono-alkynyl complexes 1a-4a have been characterized with single crystal X-ray diffraction. The cations were crystallized as the chloride (1a) or triflate (2a, 3a, and 4a) salts, and the molecular structures are shown in Fig. 1-4. Selected bond lengths and bond angles are provided in Table 1. Molecular structures for 3b and 4b are presented in Fig. S2 and S3† along with select bond lengths and angles in Table S2.† All com-

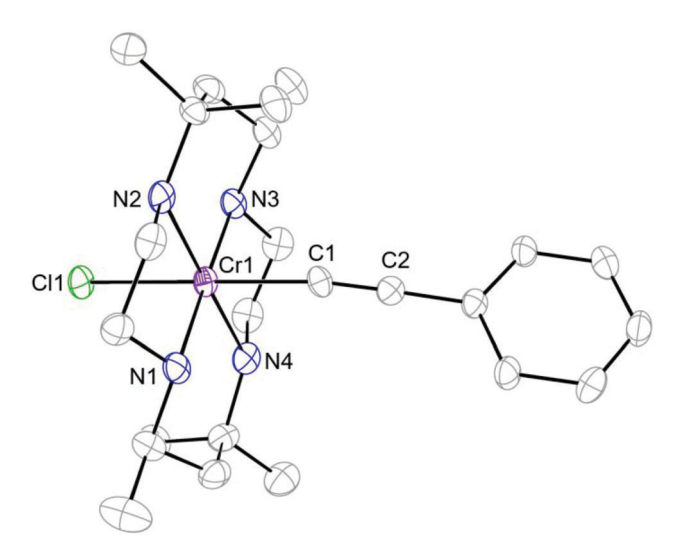


Fig. 1 ORTEP plot of $[1a]^+$ at 30% probability level. H atoms and the Cl⁻counterion were omitted for clarity.

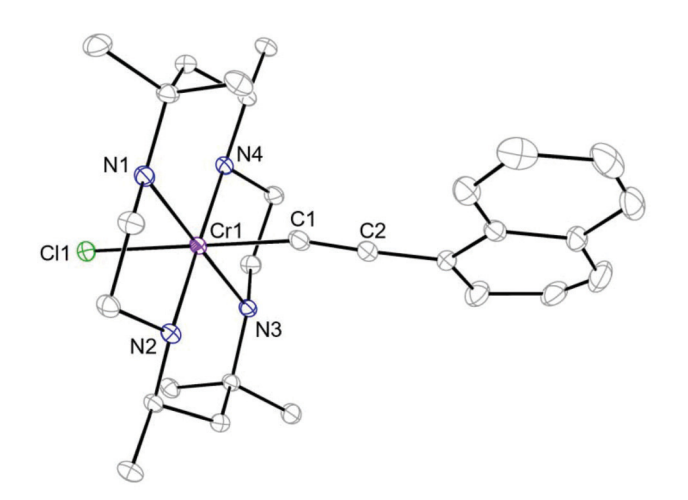


Fig. 2 ORTEP plot of [2a]⁺ at 30% probability level. H atoms, ⁻OTf counterion, and disorder were omitted for clarity.

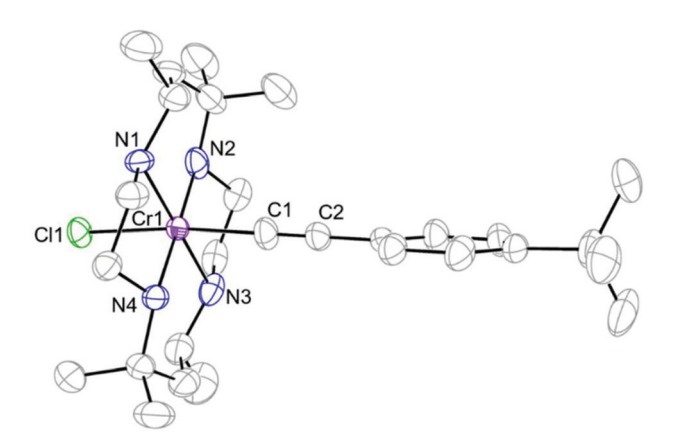


Fig. 3 ORTEP plot of [3a]⁺ at 30% probability level. H atoms, ⁻OTf counterion, and disorder were omitted for clarity.

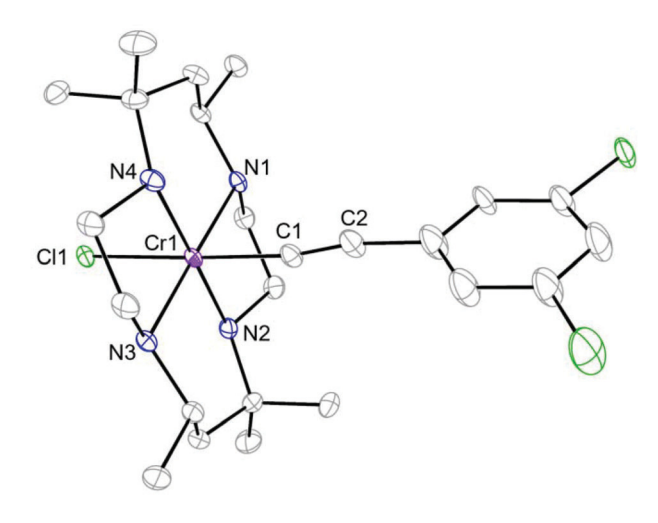


Fig. 4 ORTEP plot of $[4a]^+$ at 30% probability level. H atoms, $^-$ OTf counterion, and disorder were omitted for clarity.

Table 1 Selected bond lengths (Å) and bond angles (°) for 1a-4a

	[1a]Cl	2a	3a	4a
Cr1-N1	2.074(4)	2.077(1)	2.092(8)	2.077(2)
Cr1-N2	2.090(4)	2.096(1)	2.092(8)	2.092(2)
Cr1-N3	2.080(4)	2.074(1)	2.064(9)	2.075(2)
Cr1-N4	2.113(4)	2.088(1)	2.086(9)	2.107(2)
Cr1-C1	2.049(4)	2.035(2)	2.014(7)	2.028(2)
Cr1-Cl1	2.3678(13)	2.3704(4)	2.372(6)	2.3615(5)
C1-C2	1.205(7)	1.251(3)	1.192(4)	1.210(3)
C1-Cr1-Cl1	176.93(14)	179.81(5)	173.9(3)	178.11(7)
Cr1-C1-C2	168.1(5)	159.0(2)	174.2(4)	170.9(2)
N1-Cr1-N3	178.70(15)	171.19(5)	179.6(4)	179.11(7)
N2-Cr1-N4	179.55(16)	179.23(4)	178.3(4)	178.99(6)
N1-Cr1-N2	85.27(17)	85.15(6)	93.8(3)	84.38(4)
N1-Cr1-N4	94.85(18)	95.49(6)	84.6(4)	95.12(4)
N2-Cr1-N3	94.92(17)	94.50(7)	86.5(4)	95.28(4)
N3-Cr1-N4	84.95(18)	84.87(7)	95.2(4)	85.22(4)

plexes have pseudo-octahedral geometry and retain *trans* stereochemistry.

The Cr-C bond length of 2.049(4) Å in [1a]Cl is comparable to those observed for trans-[Cr(cyclam)(C₂Ph)₂]⁺ (avg. 2.073 Å) and 1b (avg. 2.085 Å), but slightly shortened by ca. 0.024/ 0.036 Å, respectively.^{23,37} The shorter Cr-C bond distance is not unexpected, as acetylides are stronger donors than chloro ligands, and in both trans-[Cr(cyclam)(C₂Ph)₂]⁺ and trans-[Cr (HMC)(C₂Ph)₂]Cl there is a distinct trans-influence by the two alkynyl ligands.^{23,37} A similar trend is observed for 2a with a Cr-C bond length of 2.035(2) Å, while the average of those for trans-[Cr(HMC)(C2Np)2]Cl is 2.078 Å;21 and for 4a with a Cr-C bond length of 2.028(2) Å (ca. 0.047 Å shorter than those of 4b). A more significant contrast in the Cr-C bond length is observed between 3a and 3b (ca. 0.091 Å). This is attributed to the fact that *tert*-butylphenylacetylide is the strongest σ -donor in the series and forms the strongest Cr-C bond in its monoalkynyl complex but exhibits the highest trans-influence in the bis-alkynyl complex.

Paper Dalton Transactions

The C=C bond lengths of 1a, 3a, 4a are comparable to one another, as well as to the corresponding bis-alkynyl complexes 1b, 3b, and 4b. The C=C bond length of 2a is 1.251(3) Å, which is notably longer than the observed range (1.150-1.225 Å, esd ≤ 0.010 Å) for C=C bonds in complexes containing MC=CR (R = C, Si) bonds. The ethynylnapthalene ligand in the crystal structure of 2a is disordered (Fig. S1†) and was refined to have an occupancy ratio of 0.576 (3) to 0.424(3). The disordered moiety has a C=C bond length of 1.221(4) Å, which falls within the well-established range of metal-alkynyl bonds. The disordered moiety also possesses a Cr1-C1-C2 bond angle that is in better agreement with 1a, 3a, and 4a, at $167.7(2)^{\circ}$ compared to $159.0(2)^{\circ}$ reported for 2a.

UV-vis spectroscopic analysis

The UV-vis absorption spectra of mono-alkynyl complexes 1a-4a compared to their bis-alkynyl counterparts, 1b-4b, are shown in Fig. 5–8. The absorption is assigned to the ${}^4A_{2g} \rightarrow$ ${}^4\mathrm{T_{1g}}/{}^4\mathrm{T_{2g}}$ (O_h) transition. Similar to the Cr bis-alkynyl complexes, all mono-alkynyl complexes display structured d-d bands between 300 and 450 nm for 1a, 3a, and 4a, and between 400-550 nm for complex 2a. The bathochromic shift of the metal-based absorption of 2a is a result of increased ligand aromaticity and has been previously observed. 15,22 The d-d bands of mono-alkynyl complexes are slightly red shifted from their bis-alkynyl analogues (<5 nm) due to the chloro substituent being a weaker field ligand than the arylalkynyl ligand. The intensities of these d-d bands are rather high in comparison to those seen for halide complexes trans-[Cr(HMC) X_2^{\dagger} , which reinforces the previous presumption of a partial charge-transfer character due to strong $d\pi - \pi(C \equiv C)$ mixing.²³ As shown in Fig. 5–8, the molar extinction coefficients of the d-d bands in 1a-4a are approximately half of those for their corresponding trans-[Cr(HMC)(C2Ar)2]OTf complexes, corro-

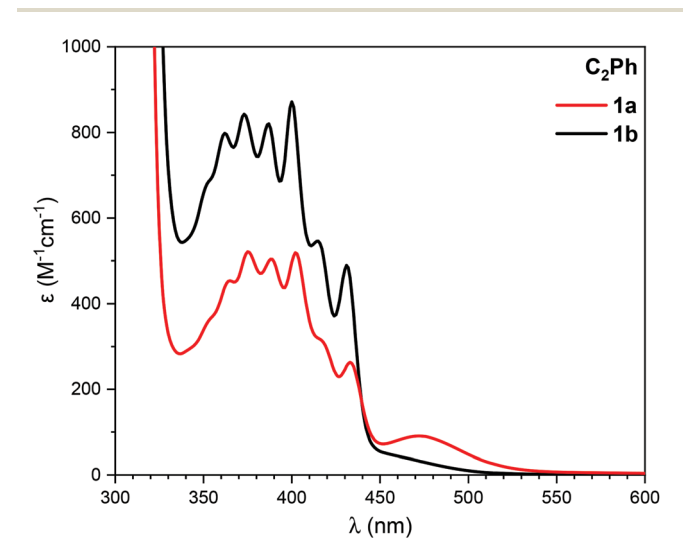


Fig. 5 UV-vis absorption spectra of complexes ${\bf 1a}$ and ${\bf 1b}$ as ${\rm CH_2Cl_2}$ solutions.

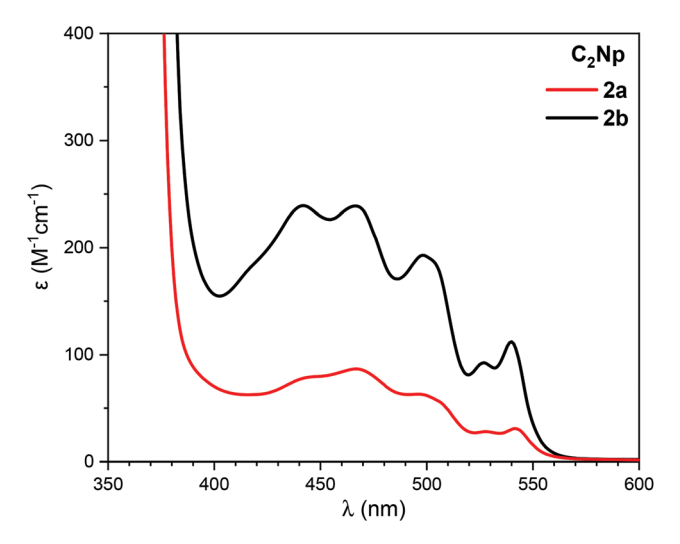


Fig. 6 UV-vis absorption spectra of complexes 2a and 2b as CH₂Cl₂ solutions.

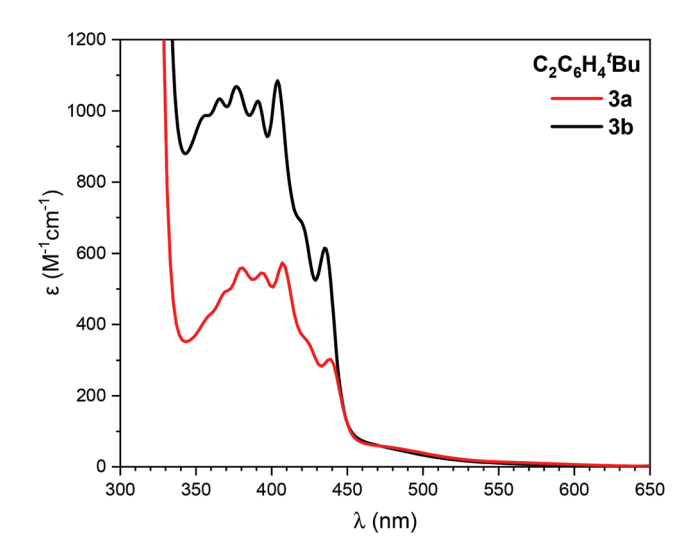


Fig. 7 UV-vis absorption spectra of complexes **3a** and **3b** as CH₂Cl₂ solutions.

borating the presumption of significant contributions from $d\pi$ – π (C=C) mixing.

Similar to the bis-alkynyl complexes, the mono-alkynyl complexes also exhibit intense absorptions below 330 nm (not shown) that are associated with charge transfer and intraligand $\pi^-\pi^*$ transitions. Also like the bis-alkynyl complexes, replacement of one of the halide ligands leads to a stronger ligand field, thus the $^4T_{1g}$ term seen for halide [Cr(HMC)X_2]^+ complexes is likely beyond the UV-vis window or hidden beneath the charge transfer bands. 23

The highly-structured nature of the d-d bands is still the most prominent feature of the spectra, and ideally, the origin of the vibronic progressions may be determined from the FT-IR of the complexes. The vibronic progressions have been calculated for 1a-4a (see Fig. S7 and Table S4†). For 1a, 3a,

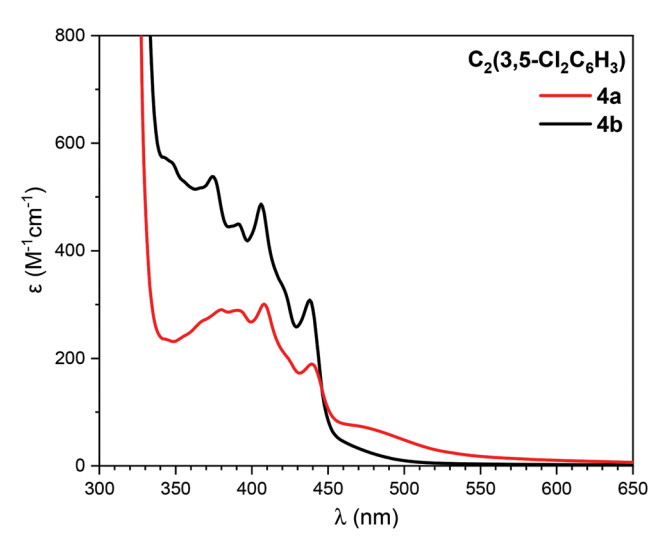


Fig. 8 UV-vis absorption spectra of complexes ${\bf 4a}$ and ${\bf 4b}$ as ${\rm CH_2Cl_2}$ solutions.

and **4a**, the progressions average between 860–980 cm⁻¹, similar to the *trans*-[Cr(HMC)(C₂Ar)₂]Cl complexes. It is difficult to determine the vibrational mode(s) responsible for the vibronic progressions due to the possible occurrence of aromatic C–H bending, N–H bending and methylene vibrations within the same region.²³ The irregularly spaced progressions for **2a** average a spacing of around 1043 cm⁻¹, which aligns more closely with aromatic C=C stretching modes or phenyl ring deformations in the Np ligand, as previously suggested for **2b**.²²

Emission studies

Complexes **1a–4a** exhibit Cr^{III} emission centered around 725 nm, as shown in Fig. 9–12. Phosphorescence in octahedral

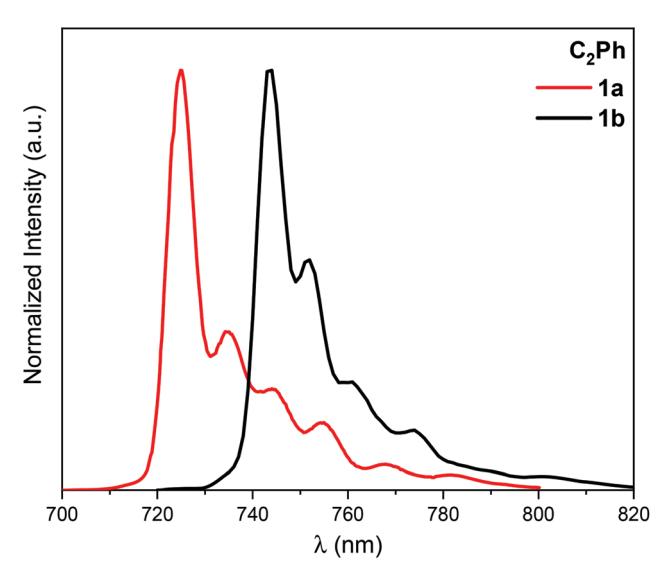


Fig. 9 Normalized emission spectra of complexes 1a and 1b in a 4:1 CH $_3$ CH $_2$ OH/CH $_3$ OH glass measured at 77 K.

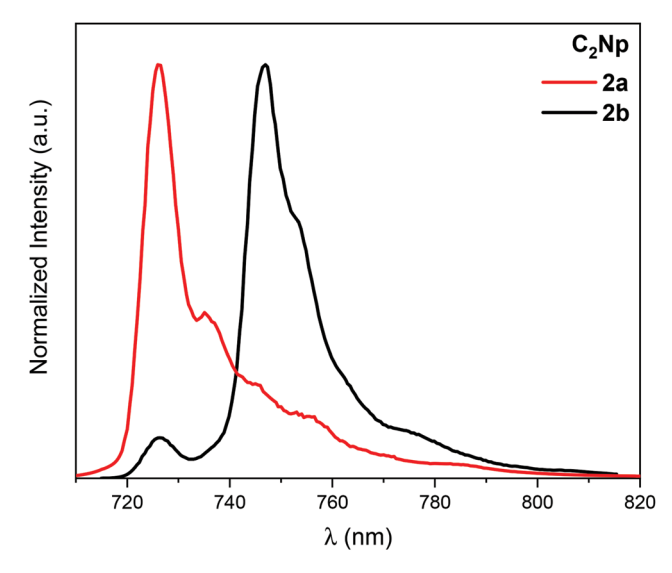


Fig. 10 Normalized emission spectra of complexes 2a and 2b in a 4:1 CH $_3$ CH $_2$ OH/CH $_3$ OH glass measured at 77 K.

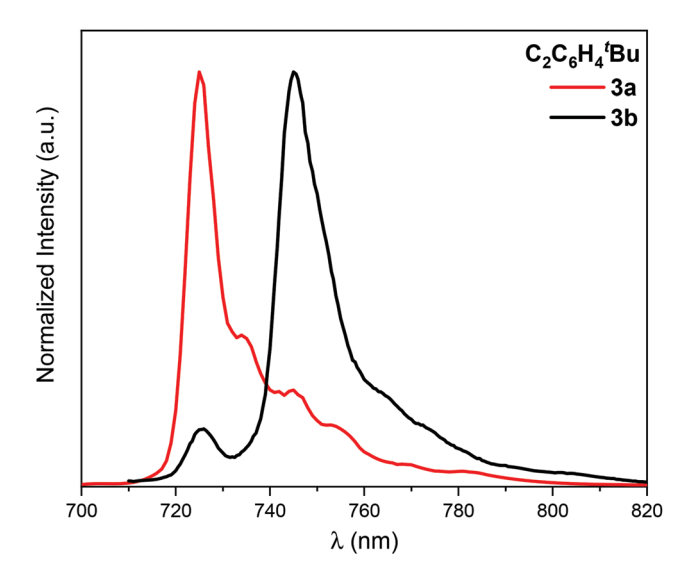


Fig. 11 Normalized emission spectra of complexes 3a and 3b in a 4:1 CH $_3$ CH $_2$ OH/CH $_3$ OH glass measured at 77 K.

 ${
m Cr^{III}}$ complexes occurs as a result of intersystem crossing from the ${}^4{
m T}_{1g}$ or ${}^4{
m T}_{2g}$ excited states to two possible lower-lying doublet states, ${}^2{
m T}_{1g}$ and ${}^2{
m E}_{\rm g}$. 39 The emission of complexes ${
m 1a}$ – ${
m 4a}$ is attributed to a ${}^2{
m T}_{1g}
ightarrow {}^4{
m A}_{2g}$ transition, which is consistent with the previous report of emissions by bis-alkynyl complexes ${
m 1b}$ and ${
m 2b}$. This assignment is partially based on the red shift from where ${}^2{
m E}_{\rm g}$ emission is usually observed. 40 The phosphorescence spectra of complexes ${
m 1a}$ – ${
m 4a}$ exhibit finestructuring at 77 K, which is believed to be vibronic in origin. 41 Stronger vibronic coupling between the alkynyl ligand and the Cr metal center results in more defined structuring of complexes ${
m 1a}$ – ${
m 4a}$ in comparison to complexes ${
m 1b}$ – ${
m 4b}$. This interpretation is supported by the shorter Cr–C bond lengths

Paper Dalton Transactions

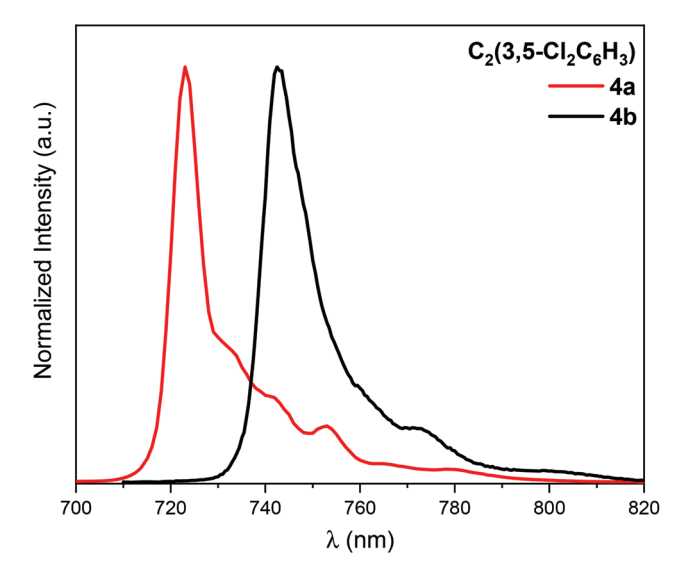


Fig. 12 Normalized emission spectra of complexes 4a and 4b in a 4:1 CH₃CH₂OH/CH₃OH glass measured at 77 K.

Table 2 Photophysical data for mono-alkynyl complexes 1a-4a and bis-alkynyl complexes 1b-4b

	Frozen glass ^a			Room temperature ^b		
	$\lambda_{\rm ex}$ (nm)	λ _{em} (nm)	τ (μs)	$\lambda_{\rm ex}$ (nm)	λ _{em} (nm)	τ (μs)
1a	400	725	397	400	725	123
2a	466	735	367	466	728	78
3a	406	725	383	406	728	87
4a	408	723	343	408	725	22
1b	425	744	469	425	746	164
2b	445	747	447	445	747	218
		727^{c}	362			
3b	403	745	479	403	748	117
		726 ^c	345			
4b	406	743	354	406	747	51

^a Measured at 77 K in a 4:1 CH₃CH₂OH/CH₃OH glass. ^b Measured at room temperature in degassed CH₃CN. ^c²E_g \rightarrow ⁴A_{2g} emission.

observed in the mono-alkynyl species. For complexes **1a-4a**, a blue shift of approximately 20 nm is observed compared to **1b-4b** (Table 2). This can be attributed to the nephelauxetic effect as the electron cloud is more localized between the Cr metal center and the alkynyl ligand in complexes **1a-4a**, resulting in higher energy emission. While the new mono-alkynyl complexes **1a-4a** display a single ${}^2T_{1g} \rightarrow {}^4A_{2g}$ emission, a weaker secondary emission of ${}^2E_g \rightarrow {}^4A_{2g}$ origin was previously noted for bis-alkynyl complex **2b** at 77 K. A secondary emission is also identified for the new bis-alkynyl complex **3b** at 726 nm.

Relevant parameters for the emissions of 1a-4a and 1b-4b are compiled in Table 2. Complexes 1a-4a have fairly long lifetimes, ranging between 343 μs to 397 μs . The lifetimes of 1b, 2b, and 3b are between 70–89 μs longer than those of 1a, 2a, and 3a, respectively. In the case of 4b, the lifetime is only $11 \mu s$ longer than that of 4a, which can likely be attributed to the

presence of two heavy chloride atoms leading to increased non-radiative decay. All four *trans* mono-alkynyl complexes have longer lifetimes than cis-[Cr(HMC)(C₂Ph)₂]Cl and cis-[Cr(HMC)(C₂Np)₂]Cl, which is unsurprising when considering that the distortions in the CN₂R₂ plane of cis-complexes often result in larger non-radiative decay rates, and thus shorter lifetimes.⁴²

Conclusion

Cr^{III} mono-alkynyl complexes supported by the HMC macrocycle have been realized with the synthesis of complexes 1a–4a, thus expanding the repertoire of Cr^{III} alkynyl chemistry. All complexes display structured d–d bands like the bis-alkynyl complexes, with approximately halved molar absorptivity values. As with the bis-alkynyl complexes, complexes 1a–4a exhibit long-lived phosphorescence at 77 K. The emission spectra of 1a–4a are more structured than their bis-alkynyl counterparts as a result of stronger vibronic coupling between the Cr^{III} metal center and the alkynyl ligand, which is supported by the mono-alkynyl complexes displaying shorter Cr–C bond lengths than their bis-alkynyl counterparts. With these mono-alkynyl complexes of Cr(HMC) being realized, synthetic efforts can be made toward dissymmetric bis-alkynyl complexes based on Cr(HMC).

Conflicts of interest

The authors have no conflicts of interest to declare.

Acknowledgements

We thank the National Science Foundation (CHE 1764347) for generously supporting this work.

References

- N. J. Long and C. K. Williams, Angew. Chem., Int. Ed., 2003, 42, 2586–2617.
- 2 M. I. Bruce and P. J. Low, Adv. Organomet. Chem., 2004, 50, 179–444.
- 3 A. Haque, R. A. Al-Balushi, I. J. Al-Busaidi, M. S. Khan and P. R. Raithby, *Chem. Rev.*, 2018, 118, 8474–8597.
- 4 M. Delor, P. A. Scattergood, I. V. Sazanovich, A. W. Parker, G. M. Greetham, A. J. H. M. Meijer, M. Towrie and J. A. Weinstein, *Science*, 2014, 346, 1492–1495.
- 5 S. D. Banziger and T. Ren, J. Organomet. Chem., 2019, 885, 39–48.
- 6 T. Ren, Chem. Commun., 2016, 52, 3271-3279.
- 7 W. A. Hoffert, M. K. Kabir, E. A. Hill, S. M. Mueller and M. P. Shores, *Inorg. Chim. Acta*, 2012, 380, 174–180.
- 8 S. N. Natoli, M. Zeller and T. Ren, *Inorg. Chem.*, 2016, 55, 5756–5758.

- 9 S. D. Banziger, X. Li, J. Valdiviezo, M. Zeller, P. Zhang, D. N. Beratan, I. V. Rubtsov and T. Ren, *Inorg. Chem.*, 2019, 58, 15487–15497.
- 10 S. D. Banziger, M. Zeller and T. Ren, Eur. J. Inorg. Chem., 2019, 4766–4772.
- 11 J.-W. Ying, A. Cordova, T. Y. Ren, G.-L. Xu and T. Ren, *Chem. Eur. J.*, 2007, **13**, 6874–6882.
- 12 R. Taube, H. Drevs and G. Marx, *Z. Anorg. Allg. Chem.*, 1977, **436**, 5–19.
- 13 L. A. Berben and J. R. Long, *J. Am. Chem. Soc.*, 2002, **124**, 11588–11589.
- 14 L. A. Berben, Ph.D. Dissertation, University of California, Berkeley, 2005.
- 15 C. Sun, C. R. Turlington, W. W. Thomas, J. H. Wade, W. M. Stout, D. L. Grisenti, W. P. Forrest, D. G. VanDerveer and P. S. Wagenknecht, *Inorg. Chem.*, 2011, 50, 9354–9364.
- 16 J. Nishijo, Y. Shima and M. Enomoto, *Polyhedron*, 2017, **136**, 35–41.
- 17 J. Nishijo and M. Enomoto, *Inorg. Chim. Acta*, 2015, 437, 59–63.
- 18 J. Nishijo and M. Enomoto, *Inorg. Chem.*, 2013, **52**, 13263–13268.
- 19 J. Nishijo, K. Judai, S. Numao and N. Nishi, *Inorg. Chem.*, 2009, **48**, 9402–9408.
- 20 W. P. Forrest, Z. Cao, R. Hambrick, B. M. Prentice, P. E. Fanwick, P. S. Wagenknecht and T. Ren, Eur. J. Inorg. Chem., 2012, 2012, 5616–5620.
- 21 E. C. Judkins, S. F. Tyler, M. Zeller, P. E. Fanwick and T. Ren, *Eur. J. Inorg. Chem.*, 2017, **2017**, 4068–4076.
- 22 E. C. Judkins, M. Zeller and T. Ren, *Inorg. Chem.*, 2018, 57, 2249–2259.
- 23 S. F. Tyler, E. C. Judkins, Y. Song, F. Cao, D. R. McMillin, P. E. Fanwick and T. Ren, *Inorg. Chem.*, 2016, 55, 8736–8743.
- 24 K. C. MacLeod, J. L. Conway, B. O. Patrick and K. M. Smith, J. Am. Chem. Soc., 2010, 132, 17325–17334.
- 25 E. W. Jandciu, J. Kuzelka, P. Legzdins, S. J. Rettig and K. M. Smith, *Organometallics*, 1999, **18**, 1994–2004.

- 26 Y.-P. Wang, H.-L. Leu, H.-Y. Cheng, T.-S. Lin, Y. Wang and G.-H. Lee, *J. Organomet. Chem.*, 2008, **693**, 2615–2623.
- 27 L. A. Berben and S. A. Kozimor, *Inorg. Chem.*, 2008, 47, 4639–4647.
- 28 W. A. Hoffert, A. K. Rappe and M. P. Shores, *Inorg. Chem.*, 2010, 49, 9497–9507.
- 29 C. Egler-Lucas, O. Blacque, K. Venkatesan, A. López-Hernández and H. Berke, *Eur. J. Inorg. Chem.*, 2012, **2012**, 1536–1545.
- 30 A. López-Hernández, K. Venkatesan, H. W. Schmalle and H. Berke, *Monatsh. Chem.*, 2009, **140**, 845–857.
- 31 R. W. Hay, N. F. Curtis and G. A. Lawrance, *J. Chem. Soc.*, *Perkin Trans.* 1, 1975, 591–593.
- 32 D. A. House, R. W. Hay and M. A. Ali, *Inorg. Chim. Acta*, 1983, 72, 239–245.
- 33 N.-h. Chang, H. Mori, X.-c. Chen, Y. Okuda, T. Okamoto and Y. Nishihara, *Chem. Lett.*, 2013, **42**, 1257–1259.
- 34 G. Brizius and U. H. F. Bunz, Org. Lett., 2002, 4, 2829-2831.
- 35 D. Lehnherr, J. M. Alzola, E. B. Lobkovsky and W. R. Dichtel, *Chem. Eur. J.*, 2015, **21**, 18122–18127.
- 36 D. F. Evans, J. Chem. Soc., 1959, 2003-2005.
- 37 D. L. Grisenti, W. W. Thomas, C. R. Turlington, M. D. Newsom, C. J. Priedemann, D. G. VanDerveer and P. S. Wagenknecht, *Inorg. Chem.*, 2008, 47, 11452–11454.
- 38 J. Manna, K. D. John and M. D. Hopkins, *Adv. Organomet. Chem.*, 1995, 38, 79–154.
- 39 N. A. P. Kane-Maguire, Photochemistry and photophysics of coordination compounds: Chromium, in *Photochemistry* and *Photophysics of Coordination Compounds I*, ed. V. Balzani and S. Campagna, Springer, Berlin, Heidelberg, 2007
- 40 A. F. Fucaloro, L. S. Forster, S. G. Glover and A. D. Kirk, *Inorg. Chem.*, 1985, 24, 4242–4246.
- 41 R. B. Lessard, M. J. Heeg, T. Buranda, M. W. Perkovic, C. L. Schwarz, R. Yang and J. F. Endicott, *Inorg. Chem.*, 1992, 31, 3091–3103.
- 42 L. S. Forster, Chem. Rev., 1990, 90, 331-353.